Bioelectrochemistry 82 (2011) 22–28

Contents lists available at ScienceDirect

Bioelectrochemistry

journal homepage: www.elsevier.com/locate/bioelechem

Structural redox control in a 7Fe ferredoxin isolated from *Desulfovibrio alaskensis*

Raquel Grazina [a,*], Patrícia M. Paes de Sousa [a], Carlos D. Brondino [b], Marta S.P. Carepo [a], Isabel Moura [a], José J.G. Moura [a,*]

[a] REQUIMTE/CQFB, Departamento de Química, Faculdade de Ciências e Tecnologia, Universidade Nova de Lisboa, 2829–516, Caparica, Portugal
[b] Facultad de Bioquímica y Ciencias Biológicas, Universidad Nacional del Litoral, S3000ZAA Santa Fe, Argentina

ARTICLE INFO

Article history:
Received 29 October 2010
Received in revised form 5 April 2011
Accepted 19 April 2011
Available online 28 April 2011

Keywords:
7Fe ferredoxins
Desulfovibrio bacteria
Iron–sulfur clusters
Electrochemistry

ABSTRACT

The redox behaviour of a ferredoxin (Fd) from *Desulfovibrio alaskensis* was characterized by electrochemistry. The protein was isolated and purified, and showed to be a tetramer containing one [3Fe–4S] and one [4Fe–4S] centre. This ferredoxin has high homology with FdI from *Desulfovibrio vulgaris* Miyazaki and Hildenborough and FdIII from *Desulfovibrio africanus*.

From differential pulse voltammetry the following signals were identified: $[3Fe\text{-}4S]^{+1/0}$ ($E^{0\prime} = -158 \pm 5$ mV); $[4Fe\text{-}4S]^{+2/+1}$ ($E^{0\prime} = -474 \pm 5$ mV) and $[3Fe\text{-}4S]^{0/-2}$ ($E^{0\prime} = -660 \pm 5$ mV). The effect of pH on these signals showed that the reduced $[3Fe\text{-}4S]^{0}$ cluster has a $pK'_{red} = 5.1 \pm 0.1$, the $[4Fe\text{-}4S]^{+2/+1}$ centre is pH independent, and the $[3Fe\text{-}4S]^{0/-2}$ reduction is accompanied by the binding of two protons. The ability of the $[3Fe\text{-}4S]^{0}$ cluster to be converted into a new [4Fe–4S] cluster was proven. The redox potential of the original [4Fe–4S] centre showed to be dependent on the formation of the new [4Fe-4S] centre, which results in a positive shift (*ca.* 70 mV) of the redox potential of the original centre.

Being most [Fe–S] proteins involved in electron transport processes, the electrochemical characterization of their clusters is essential to understand their biological function. Complementary EPR studies were performed.

1. Introduction

Ferredoxins (Fds) are iron-sulfur proteins that act as electron carriers in metabolic processes such as N_2 and CO_2 fixation, sulphate reduction and biodegradation [1–3]. This type of proteins can be found in different sources such as bacteria, plants and mammals and are subdivided in different classes according to the type and the number of their [Fe-S] clusters. The [2Fe–2S] centres can be found in plants and animals whereas the [3Fe–4S] and [4Fe–4S] centres are typically found in bacteria. Moreover, the bacterial ferredoxins also contain two types of aggregates: [3Fe–4S] + [4Fe–4S] or 2 × [4Fe–4S], corresponding to the 7Fe and 8Fe ferredoxins, respectively. The amino acid sequence of 7Fe ferredoxins isolated from *Desulfovibrio (D.)* genus contains seven cysteine residues involved in the binding of both clusters. The [4Fe–4S] cluster binding domain is highly conserved and contains the cysteine-rich sequence: Cys^{I}-Xaa_2-Cys^{II}-Xaa_2-Cys^{III}-Xaa_n-Cys^{IV}-Pro called the "classic" [4Fe–4S] cluster binding motif. The [3Fe–4S] cluster binding domain is similar but requires only a minimum of three coordinating ligands, which are usually cysteine residues I, III and IV. However, in the particular case of *Desulfovibrio africanus* ferredoxin III (*Da*FdIII) and *Desulfovibrio vulgaris* Miyazaki ferredoxin I (*Dv*MFdI) the Cys^{II} of the 3Fe centre binding motif is replaced by an aspartic acid residue [4,5]. It was shown that the replacement of the Cys residue by an aspartate in the cluster binding motif leads to the rapidly and reversibly uptake of another iron atom by the 3Fe centre to produce a 8Fe ferredoxin. The same behaviour was also demonstrated by the [3Fe–4S] cluster of other Fds such as *Desulfovibrio gigas* FdII, but in this case the protein has the usual and classic binding motif [6,7].

Electrochemical techniques are powerful tools for the analysis of metalloproteins due to the possibility of obtaining important information about the intrinsic thermodynamic and kinetic properties of these systems, in particular when direct electron transfer (DET) is achieved. Protein film voltammetry (PFV) and membrane electrodes are two particularly interesting strategies for DET, since very small sample amounts are required, sluggish diffusion of the protein is avoided and investigations over a wide range of experimental conditions are easily performed [8,9].

The [Fe–S] clusters of 7Fe ferredoxins, in particular *Da*FdIII, have been characterized by voltammetric methods with the protein either in solution or adsorbed at the electrode surface and these studies showed the presence of three distinct redox couples: $[3Fe\text{-}4S]^{+1/0}$ ($E^{0\prime} = -140$ mV); $[4Fe\text{-}4S]^{+2/+1}$ ($E^{0\prime} = -410$ mV) and $[3Fe\text{-}4S]^{0/-2}$ ($E^{0\prime} = -726$ mV) at pH *ca.* 7 [4,10,11]. These studies also indicate that, when reduced, the [3Fe-4S] cluster centre reacts with Fe(II) ions to form a product having a redox potential very similar to that of the original [4Fe–4S] cluster. The magnetic properties of the [Fe–S] clusters in different redox states have also been evaluated by EPR and MCD spectroscopies [4,10,12] and these data showed that the 4Fe cluster in its

* Corresponding authors. Tel.: +351 212948381; fax: +351 212948550.
E-mail addresses: raquel.grazina@dq.fct.unl.pt (R. Grazina), jose.moura@dq.fct.unl.pt (J.J.G. Moura).

1567-5394/$ – see front matter © 2011 Elsevier B.V. All rights reserved.
doi:10.1016/j.bioelechem.2011.04.005

$[4Fe–4S]^{+2}$ form is diamagnetic, while $[4Fe–4S]^{+1}$ is paramagnetic with the ground state being $S=1/2$ ($g_{max}=2.05$, $g_{mid}=1.93$, $g_{min}=1.89$). The 3Fe clusters in the $[3Fe–4S]^{+1}$ and $[3Fe–4S]^{0}$ forms are both paramagnetic and give rise to EPR signals at $g\sim2.01$ ($S=1/2$) and $g\sim12$ ($S=2$), respectively. The EPR spectra of these proteins also show a signal at $g\sim5$, which was assigned to a $[4Fe–4S]^{+1}$ cluster in a $S=3/2$ spin configuration. This signal is associated with $[4Fe–4S]^{+1}$ clusters that result from the reaction of $[3Fe–4S]^{0}$ clusters with Fe(II) ions. However, this signal is not observed when the Aspartate (Asp^{15}) residue is mutated to a Cysteine residue, demonstrating that the cluster conversion is associated with this residue [13].

In this work a 7Fe ferredoxin was isolated for the first time from the sulphate reducing bacterium *Desulfovibrio alaskensis* (*Dalask*Fd), a bacterium recovered from a soured oil well in Purdu Bay, Alaska [14]. The characterization of this protein identified some common features observed in other 7Fe ferredoxins but also shows intrinsic characteristics. The biochemical, electrochemical and spectroscopic (EPR) characterization of this protein is reported and its properties are discussed in comparison with 7Fe ferredoxins from other sources.

2. Material and Methods

2.1. Growth Conditions and Purification Procedures

D. alaskensis NCIMB 13491 was grown at 37 °C in Postgate C medium under anaerobic conditions in the Unite de Fermentation at LCB-CNRS in Marseille, France, and cells were harvested at the logarithmic/early stationary phase of bacterial growth. The cells were lysed using a Maunton-Gaulin French press (15000 psi).

All the purification procedures were performed aerobically at 4 °C and using Tris-HCl buffer pH 7.6. At each purification step the protein purity was evaluated by UV-visible spectroscopy and 15% Tris–glycine SDS–PAGE. The purification procedure started with the centrifugation of the cell extract of *D. alaskensis* at 9900 *g* for 30 min, followed by ultracentrifugation of the supernatant at 180000 *g* for 60 min to remove the membrane fraction. The soluble extract was then dialyzed overnight against 5 mM Tris–HCl buffer and loaded onto a DEAE-52 Whatman column (38×5.5 cm ∅) equilibrated with the same buffer. A Tris-HCl buffer linear gradient (5–500 mM) was applied, the fraction containing the ferredoxin was collected at an ionic strength range between 450 and 500 mM and then dialyzed against 100 mM Tris–HCl buffer. The second purification step was performed using a DEAE Sepharose Fast Flow column (22×2.6 cm ∅), which was previously equilibrated with 100 mM Tris-HCl buffer. The ferredoxin sample was eluted at a flow rate of 3 mL/min using a Tris-HCl buffer linear gradient (100–500 mM). The sample was again loaded onto an anionic exchange column (Q-Resource, 6 mL) equilibrated with 10 mM Tris-HCl, and followed by a Tris–HCl buffer linear gradient (10–600 mM) at a flow rate of 3 mL/min. The fraction containing ferredoxin was collected at an anionic strength *ca.* 450 mM and concentrated in a Diaflow apparatus over a YM5 membrane. Finally, as the last purification step, a size-exclusion chromatography was performed using a Superdex 75 (GE Healthcare) column (52×2.6 cm ∅), equilibrated with 300 mM Tris–HCl buffer and eluted in the same buffer at a 3 mL/min flow rate.

2.2. Protein and Metal Quantification

For protein quantification, a Bicinchoninic Acid kit (Sigma) was used, with a bovine serum albumin protein solution (1 mg/mL) as the standard. The iron content in the protein solution was determined by Inductively Coupled Plasma Emission Analysis (ICP) in a Jobin–Yvon (Ultima) instrument, using the Reagecon 23 ICP multielements as standard solution (100 ppm in 5% HNO_3 and 0.2% HF) in a concentration range between 0.05 and 3 ppm.

2.3. Molecular Mass Determination

The molecular mass of the ferredoxin as-isolated was determined by size-exclusion chromatography using a Superdex 75 column from Pharmacia (30×1 cm ∅) equilibrated with 50 mM Tris–HCl and 150 mM NaCl buffer (pH 7.6) with a flow rate of 0.3 mL/min. A total volume of 100 μL of the protein sample or standards was applied onto the column. The protein standards (kg/mol) were: aprotinin (6.5), ribonuclease A (13.7), carbonic anhydrase (29), ovalbumin (43) and conalbumin (75) from Amersham Pharmacia.

The molecular mass of ferredoxin was analyzed by electrospray mass spectrometry using a Bruker Microtof ESI-TOF spectrometer.

2.4. N-Terminal and DNA sequencing

The *N*-Terminal sequence was determined by automated Edman degradation in an Applied Biosystems protein sequencer model 491 coupled to an Applied Biosystem 120 analyzer according to the manufacturer´s instructions. For the DNA sequencing, two primers were designed based on *D. desulfuricans* strain G20 genome sequence that encodes the gene annotated as FdI (60 base pairs upstream and 34 downstream the target gene), since the *D. alaskensis* genome is not available in the data base and the two strains are probably subspecies or different strains from the same species [15,16]. The designed primers were the following: 5'-GGCGCGGTTTACAAAAATC-3' (upstream) and 5'-AGCATGTCGCGTATGCTTG-3' (downstream). Direct PCR of boiled *D. alaskensis* cells suspension allowed rapid amplification of the selected sequence that encodes the FdI gene. The cells (25 μL) were resuspended in 30 μL of water and the suspension was kept in a boiling water bath for 10 min, followed by centrifugation at 10,000 rpm for 10 min. A volume of 4 μL of supernatant was used as DNA template and NZYPremium DNA polymerase (NZYTech) was used in the amplification reaction. The PCR was carried out in a thermal cycler (Biometra) using the following program: 95 °C during 5 min, 30 cycles of 1 min at 95 °C for denaturation, followed by 40 s at 56 °C for the annealing and 1 min 20 s at 72 °C for elongation. After these cycles the mixture was incubated for 10 min at 72 °C for final DNA extension and cooled down to 4 °C. The PCR product was analyzed in 1% agarose gel, showing a fragment with approximately 0.3 kbp which was purified using a QIAquick extraction kit (Qiagen). The DNA fragment was directly sequenced using an ABI3700 DNA analyzer (Perkin-Elmer/Applied Biosystems, Stabvida, Caparica, Portugal).

The BLAST program at NCBI [17] was used for sequence data base searching and the CLUSTALW program was used to perform and generate multiple protein alignments [18].

2.5. Electrochemichal Studies

The electrochemical studies were performed by differential pulse (DP) voltammetry using a potentiostat/galvanostat AUTOLAB/PGSTAT30 and data analysed with the GPES software package, both from ECO Chemie. All the experiments were performed in a potential window between 0.1 V and −0.8 V vs. SHE. The pulse amplitude (ΔE) was 50 mV and the potential increment at each pulse was 5 mV. The pulse width (t_p) was changed between 20 ms and 100 ms. The electrochemical cell was constituted by an Ag/AgCl reference electrode (205 mV vs. SHE), a platinum counter electrode and a pyrolytic graphite edge (PGE) working electrode. Throughout the paper all potential values are referred to the standard hydrogen electrode (SHE). The studies were performed at room temperature and the supporting electrolyte was always deaerated for 30 min before each experiment using an argon flow.

In all sets, the PGE electrode was previously polished with several alumina supensions (1 μm, 0.3 μm and 0.05 μm) on a polishing cloth, rinsed well with Milli-Q water and finally sonicated for 10 min to

remove all the Al_2O_3 traces. The protein solution (3 μL) was entrapped between the PGE electrode and a dialysis membrane (negatively charged Spectra/Por MWCO 3500), in the membrane electrode configuration [9].

Both the supporting electrolyte and the working solution contained 50 mM MES buffer pH 6.5, 100 mM NaCl and 2 mM EGTA. Protein in a 150 μM concentration and 0.2 mg/mL polymyxine were also present in the working solution. Before preparing this solution, the protein was dialyzed against 2 mM EGTA, to remove all traces of adventitious iron.

The pH studies were performed in the range 4–8, by adding to the supporting electrolyte small aliquots of concentrated NaOH or HCl solutions, which were dispensed onto the solution trough a syringe coupled to the electrochemical cell. A Crison pH meter electrode was used. The supporting electrolyte contained 100 mM NaCl, 2 mM EGTA and a mixture of the following buffer solutions: 50 mM acetate, 50 mM MES and 50 mM HEPES.

For the reaction between *Dalask*Fd and Fe(II) ions, several aliquots of a freshly prepared 200 mM $Fe(NH_4)_2(SO_4)_2.6H_2O$ solution were added to the supporting electrolyte, corresponding to the following concentrations of Fe(II) in solution (mM): 0.05, 0.1, 0.2, 0.3, 0.5, 0.7, 0.9, 1 and 2.

2.6. EPR Spectroscopy

Continuous wave X-band EPR spectra were recorded on a Bruker EMX spectrometer equipped with a rectangular cavity model (ER 4102ST) using a 100 kHz field modulation and an Oxford Instruments continuous-flow cryostat. The protein samples (300 μM in Tris-HCl 100 mM, pH 7.6) as-isolated and reduced, using either sodium dithionite or titanium(III) citrate, were measured at 4.8 K. Both reducing agents were prepared and added to the protein sample in an anaerobic glovebox. Titanium(III) citrate solution was prepared as described elsewhere [19]. *g*-Factors were calculated from the resonance condition:

$$g = \frac{h\nu}{\beta B}$$

where h is the Planck constant, ν the microwave frequency, β the Bohr magneton and B the magnetic field.

3. Results and Discussion

3.1. Purification of DalaskFd, UV–visible Spectrum, Metal Content and Molecular Mass

As previously described in section 2.2, *Dalask*Fd was purified in four chromatographic steps. The UV-visible spectrum of the as-isolated pure protein shows two absorption bands at 280 nm and 408 nm and a shoulder around 305 nm (Fig. 1), which is in agreement with the results obtained for other 7Fe ferredoxins [20]. The electrophoretic pattern of the denaturating gel shows a unique band (inset on Fig. 1) around 6.9 kDa.

The measurements of the iron content in the *Dalask*Fd solution showed that the average extinction coefficient per iron atom was $\varepsilon_{408} = (4200 \pm 200)\,M^{-1}\,cm^{-1}$ or $\varepsilon_{408} \approx (29{,}400 \pm 1400)\,M^{-1}\,cm^{-1}$ per monomer. This value is similar to the molar extinction coefficient previously determined for the 7Fe atoms ferredoxin from *D. africanus* ($\varepsilon_{408} = 28{,}600\ M^{-1}\,cm^{-1}$) [21].

The ESI-TOF mass spectrum of *Dalask*Fd showed a unique peak corresponding to a molecular mass of 6677.68 ± 0.05 Da. The molecular weight of the as-isolated protein obtained by size-exclusion chromatography was 23 ± 2 kDa, indicating that as-purified DalaskFd is a homotetramer.

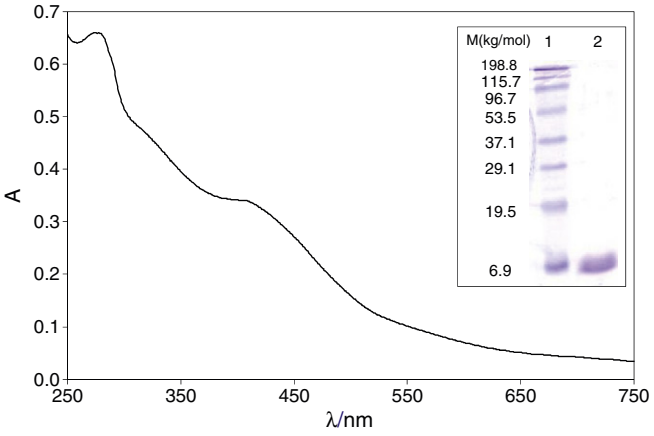

Fig. 1. UV–visible spectrum of *Dalask*Fd in 100 mM Tris-HCl pH 7.6. Inset: 15% Tris–glycine SDS-PAGE of *Dalask*Fd; lane1: protein molecular mass markers (kg/mol); 198.8, 115.7, 96.7, 53.5, 37.1, 29.1, 19.5 and 6.99; lane 2: as-purified *Dalask*Fd.

3.2. N-terminal and DNA Sequence Analysis

The BLASTP search revealed that the *N*-terminal amino acid sequence (16 amino acids sequenced) of the as-purified *Dalask*Fd (GWNVTVDHDKCTGDGE) presents 100% identity with the FdI from *D. desulfuricans* G20. This high sequence homology is due to the fact that *D. alaskensis* and *D. desulfuricans* are probably subspecies or different strains from the same species [15,16]. The DNA sequence of *Dalask*Fd (189 bp) shows 100% identity with the corresponding genes from *D. desulfuricans* G20 FdI. In Fig. 2 the multiple alignment of the deduced *Dalask*Fd amino acid sequence is represented, together with the amino acid sequence of other three ferredoxins from *D.* genus. The blast search of this deduced amino acid sequence showed a strong homology of *Dalask*Fd with *Dv*MFdI (88% identity) and *Dv*HFdI (86% identity) and also with *Da*FdIII (81% identity) (see Fig. 2). The analysis of these sequences shows that *Dalask*Fd protein is constituted by 62 amino acid residues, including the 7 cysteines usually involved in the clusters binding. The central residue in the sequence involved in the coordination of the [3Fe–4S] cluster (Cys^{12}-Xaa-Xaa-Cys^{15}-Xaa-Xaa-Cys^{18}), is in general a conserved cysteine residue (Cys^{15}). In the case of *D. gigas* FdII, this cystein is non coordinated at the 3Fe centre but has an important role in the interconversion process becoming a ligand of the 4Fe centre [21]. In the case of *Dalask*Fd, as well as for the homologous ferredoxins, an aspartic acid residue is present in this position. This replacement can contribute for the easy metal uptake by the cluster since an aspartate ligand is more labile than a cysteine, as previously demonstrated in the studies with native and mutated *Da*FdIII [13]. The same consensus sequence of Cys-Xaa-Xaa-Asp-Xaa-Xaa-Cys was also found in bacterial ferredoxins from *Pyrococcus furiosus*, *Sulfolobus acidocaldarius* and *Thermoplasma acidophilum*, which are less homologous to the ones represented herein [22–24].

3.3. Electrochemical Studies

The electrochemical behaviour of *Dalask*Fd was analysed at a PGE membrane electrode by differential pulse (DP) voltammetry. Typical DP voltammograms of the protein treated with EGTA (see Materials and Methods) exhibit three peaks (Fig. 3). At a membrane electrode, thin layer conditions are verified as long as the film thickness (l) is smaller than the diffusion layer thickness for a given experimental time scale (t), i.e. $l < (2Dt)^{1/2}$ [25], where D is the diffusion coefficient of the redox species. Although experimental conditions such as the electrode preparation may influence the thickness of the entrapped solution layer, it has been shown that reproducible layers are obtained for a series of independent experiments [9]. Typically, the value of l is

```
DalaskFd  MGWNVTVDHDKCTGDGECVDVCPVEVYELQDGKAAVVNEEECLGCESCVEVCESDAITIEEV 62
DvMFdI    MGWTVTVDTDKCTGDGECVDVCPVEVYELQDGKAVPVNEEECLGCESCVEVCEAGALTVEEN 62
DvHFdI    MGWTVTVDTDKCTGDGECVDVCPVEVYELQDGKAVAVNEEECLGCESCVEVCEAGALTVEEN 62
DafFdIII  MGYKITIDTDKCTGDGECVDVCPVEVYELQDGKAVAVNEDECLGCESCVEVCEQDALTVEEN 62
          **:.:*:* ************************. ***:************* .*:*:**
```

Fig. 2. Multiple sequence alignment between ferredoxin from *D. alaskensis* (*Dalask*Fd), ferredoxin I from *D. vulgaris* Miyazaki (*Dv*MFdI), ferredoxin I from *D. vulgaris* Hildenborough (*Dv*HFdI) and ferredoxin III from *D. africanus* (*Da*FdIII). Dark grey (*) identity; Light grey (:) strongly similar and (.) weakly similar. In bold are marked the cysteine residues.

around 10^{-3} cm. The diffusion coefficient of ferredoxin can be estimated with the equation $D = 3.3\times10^{-5}/(PM)^{1/3}$[26] (where PM is the molar mass of the protein), valid for spherical molecules with high molar mass. A D value of 1.7×10^{-6} cm^2 s^{-1} was estimated, which corresponds to a diffusion layer thickness of *ca.* 6×10^{-4} cm for the longest time scale used, $t_p = 100$ ms. Thus, the diffusion layer thickness is always smaller than l in our experimental conditions, and hence the analysis of the voltammograms should be performed in terms of a diffusion-controlled process.

In that conditions, a linear variation of the peak current (i_p) with $(1/t_p)^{1/2}$ is expected ($(\delta i)_{max} \equiv i_p = nFAC\,(D/(\pi t_p))^{1/2}\,((1-\sigma)/(1+\sigma))$ [25]), and this correlation was verified for the three signals. The equations obtained for these plots are: $i_p = -7.73\times10^{-8}\,(1/t_p)^{1/2} + 2.08\times10^{-7}$, $r = 0.996$ (signal 1); $i_p = -1.05\times10^{-7}\,(1/t_p)^{1/2} + 3.13\times10^{-7}$, $r = 0.993$ (signal 2); $i_p = -1.72\times10^{-7}\,(1/t_p)^{1/2} + 4.36\times10^{-7}$, $r = 0.998$ (signal 3). Moreover, in all cases the peak potentials remained constant for all pulse widths. The peak width at half height was also constant for the three signals in the whole time scale used, with values of $W_{1/2}\,(1) = 95\pm5$ mV, $W_{1/2}\,(2) = 112\pm5$ mV and $W_{1/2}\,(3) = 67\pm5$ mV. These features indicate that a reversible redox process is responsible for each signal. Therefore, both the formal reduction potential ($E^{0'}$) and the number of electrons involved (n) can be estimated. The former is calculated based on the peak potentials and the pulse amplitude, $E^{0'} \equiv E_{1/2} = E_p + \Delta E/2$ [24]. Formal reduction potentials of $E^{0'}\,(1) = -158\pm5$ mV, $E^{0'}\,(2) = -474\pm5$ mV and $E^{0'}\,(3) = -660\pm5$ mV were estimated, at pH 6.5. In the case of the number of electrons, its determination is based on the $W_{1/2}$ values. Since a width of 89/n mV is expected for a reversible system at 20 °C [25], peak 1 and 2 must correspond to one-electron transfer reactions, whereas in peak 3 a two-electron process is occurring. This is also evidenced by the plots (i_p) vs. $(1/t_p)^{1/2}$, since similar slopes were obtained for peaks 1 and 2 whereas for peak 3 this value is approximately the double.

By integrating the area under the peaks in the voltammograms, the charge transferred during each reduction process, Q, was calculated. This charge is proportional to the number of molecules reduced and electrons exchanged, and so the ratio between the values corresponding to each process is an indication of the relationship between the electroactive species. The ratio Q(2)/Q(1) was always around 1, whereas the ratios Q(3)/Q(1) and Q(3)/Q(2) lied close to 2, confirming that the same number of electrons are exchanged in processes 1 and 2, while in process 3 this number is the double.

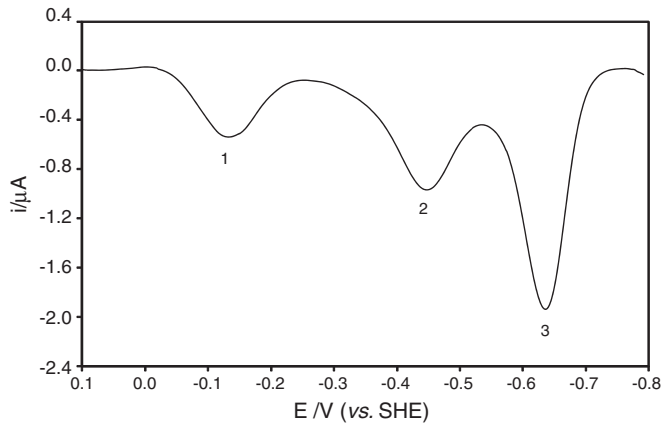

Fig. 3. DP voltammogram ($t_p = 20$ ms) of 150 μM *Dalask*Fd at a PGE membrane electrode, in the presence of 0.2 mg/mL polymixine. Medium: 5 mM MES buffer pH 6.5 and 100 mM NaCl.

According to the results reported in the literature for other 7Fe ferredoxins [11,27], the signals observed in the voltammograms of *Dalask*Fd can be assigned to the following redox processes: $[3Fe\text{–}4S]^{+\,1/0}$ (signal 1), $[4Fe\text{–}4S]^{+\,2/+1}$ (signal 2) and $[3Fe\text{–}4S]^{0/-2}$ (signal 3). The formal reduction potentials estimated for these processes are similar to the values determined for homologous proteins at the same pH, in particular the E^0 of the couples $[3Fe\text{–}4S]^{+\,1/0}$ and $[3Fe\text{–}4S]^{0/-2}$ in *Da*Fd III (−142 and −670 mV, respectively [28]) and the $E^{0'}$ of $[4Fe\text{–}4S]^{+\,2/+1}$ in *Dv*MFdI (−440 mV [27]).

The $[3Fe\text{–}4S]^0$ centre seems to have a strong tendency to spontaneously convert to $[4Fe\text{–}4S]^{+\,2}$ upon reduction since, even with EGTA present, the width of signal 2 is higher than the expected value for a one-electron process in the first scan and the peak gets broader with time (in consecutive scans). In the case of signal 3, the deviation of $W_{1/2}$ from the predicted value (45 mV) may reflect a certain degree of incomplete concertedness of the two reduction processes.

The effect of the pH on the electrochemical signals detected for *Dalask*Fd was analysed. The pH was varied between 4 and 8 and the profiles obtained for signals 1 and 3 can be observed in Fig. 4. Signal 2 showed to be pH independent.

In the case of signal 1 the pH effect observed (Fig. 4(A)) corresponds to the following set of equilibria [29]:

$$[3Fe-4S]^{+\,1}R + e^- \rightleftharpoons [3Fe-4S]^0R + H^+ \overset{K'_{red}}{\rightleftharpoons} [3Fe-4S]^0RH^+$$

where R is an aminoacid residue in the vicinity of the centre and K'_{red} is the apparent proton dissociation constant of the reduced form. Data were fitted to the equation [29]:

$$E^{0'} = E^{0'}_{alk} + (RT/nF)\ln\left(\left(K'_{red} + \left[H^+\right]\right)/K'_{red}\right) \quad (1)$$

where $E^{0'}$ is the measured reduction potential and $E^{0'}_{alk}$ is the reduction potential at high pH. Least squares fitting of the data (with no fixed parameters) yielded $E^{0'}_{alk} = -170\pm2$ mV and $pK'_{red} = 5.1\pm0.1$.

This proton uptake of the reduced state $[3Fe\text{–}4S]^0$ has been reported for other 7Fe ferredoxins [28,30–32], in particular for the highly homologous protein from *D. africanus* for which a p*K′* of 4.9 was estimated [28]. The exact site of proton binding has not been determined conclusively, but it is most likely one of the μ-sulfido ligands of this cluster [33,34]. Moreover, spectroscopic and electrochemical studies of *A. vinelandii* FdI revealed that the adjacent aspartate residue plays a central role in this proton transfer mechanism [35,36].

In the case of signal 3, a linear dependency of the redox potential with pH is verified (Fig. 4(B)) with a slope 67 ± 3 mV, consistent with a transfer ratio $H^+/e^- = 1$. This is in agreement with the behaviour observed for other 7Fe ferredoxins, including the *Da*FdIII, where a concomitant uptake of two protons and two electrons by the $[3Fe\text{–}4S]^0$ cluster showed to be essential for the formation of the species $[3Fe\text{–}4S]^{-2}$[11,28].

The possible conversion of the [3Fe–4S] cluster into a new [4Fe–4S] was probed for *Dalask*Fd by tracing DP voltammograms in the presence of increasing Fe(II) concentrations (Fig. 5).

It is clear from Fig. 5 that the addition of increasing Fe(II) concentrations results in a shift of peak 2 and a simultaneous decrease

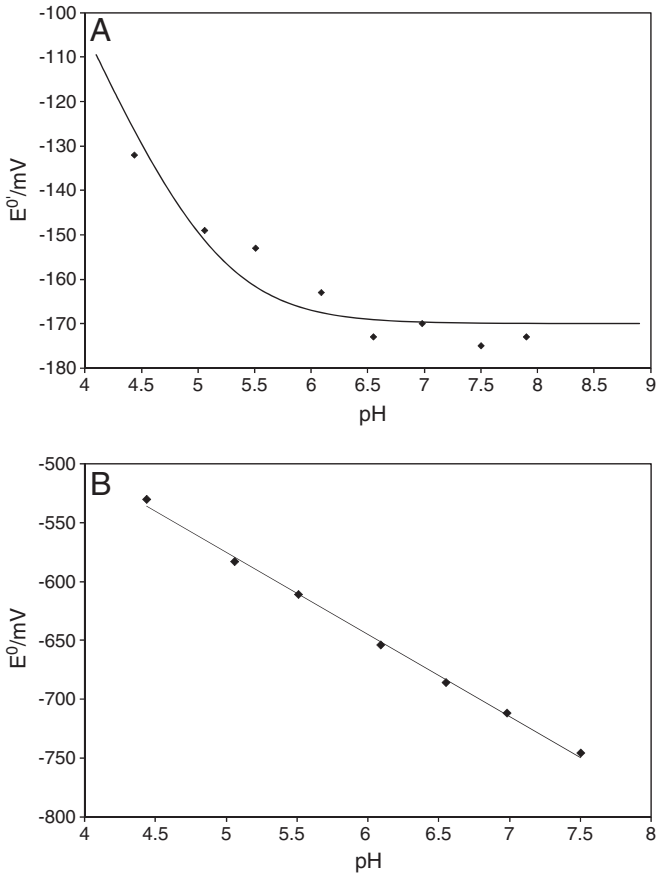

Fig. 4. Effect of pH on the reduction potential of signal 1 (A) and signal 3 (B) of *Dalask*Fd. Data fitted with Eq.1 in (A), with $E^{0'}_{alk} = -170$ mV and p$K = 5.1$. Data linearly fitted in (B) with $E^{0'} = (-67 \pm 3)\ pH + (-242 \pm 18)$.

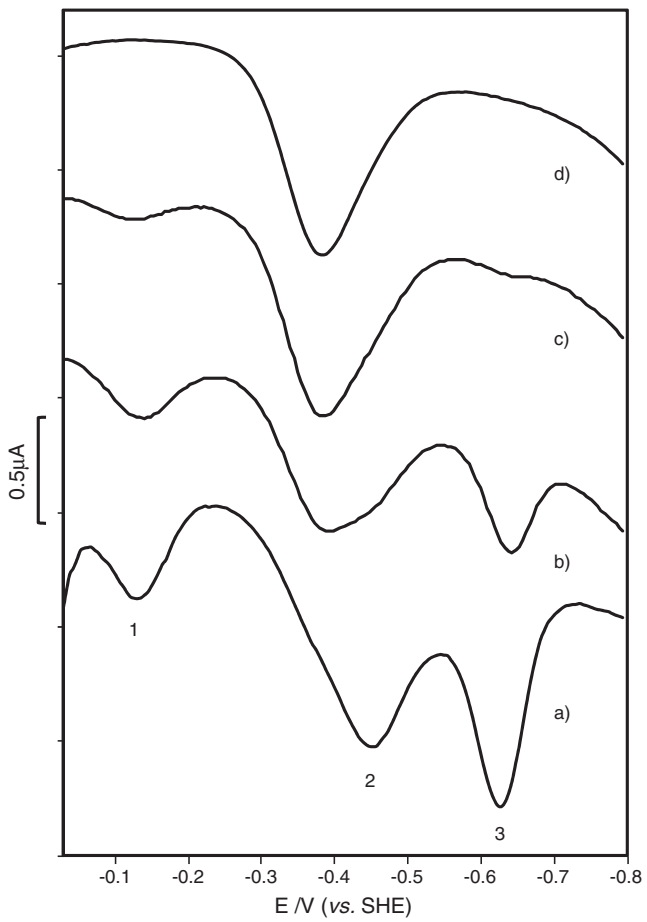

Fig. 5. DP voltammograms of *Dalask*Fd at a PGE membrane electrode with increasing in 5 mM MES buffer, 100 mM NaCl, pH 6.5, and 0.2 mg/mL polymyxine). (a) without Fe(II) ions, (b) 0.05 mM, (c) 0.5 mM and (d) 2 mM.

of peaks 1 and 3. In the presence of 2 mM Fe(II) in solution (Fig. 5(d)), the latter are no longer observed and only a peak with $E^{0'} = -408$ mV vs. SHE and $W_{1/2} = 122$ mV is detected. These observations indicate that, as for other 7Fe ferredoxins, the $[3Fe\text{–}4S]^{+1/0}$ centre, when reduced, rapidly reacts with Fe(II) ion to form a $[4Fe\text{–}4S]^{+2}$ cluster. As evidenced in Fig. 5 (b), the redox potential of the converted centre is *ca.* 70 mV more positive than that of the original 4Fe cluster ($E^{0'} = -474$ mV vs. SHE). Moreover, along the conversion process the potential of the original cluster is positively shifted and in the end the redox potentials of both $[4Fe\text{–}4S]^{2+/1+}$clusters are identical (Fig. 5(d)). The redox potential of the original [4Fe–4S] centre seems to depend on the formation of the new [4Fe–4S] centre, and this interaction may be associated with a major efficiency in the electron transfer process in which these proteins are involved. A potential shift was also reported for *Da*FdIII, but in this case a smaller difference was observed (*ca.* 10 mV) [10]. It is known that the nature of the [Fe–S] cluster surroundings influences the potential of the redox couples. In this context, some of the most important factors are solvent exposure, formation of new NH–S bonds with the cluster and the presence of charged residues in its vicinity. According to structural data for 7Fe ferredoxins, the amino acid residue in position 2 is on the protein surface and close to the [4Fe–4S] cluster and its nature has shown to be relevant for the redox properties of this cluster [37,38]. In *A. vinelandii* FdI no change in $E^{0'}$ was observed after the mutation F2Y, whereas the F2H mutation increased the redox potential by +105 mV. This shift was attributed to the introduction of a positive charge in the vicinity of the cluster due to the Histidine protonation [37]. In *Dalask*Fd and *Da*FdIII residue 3 (position 2 in *A. vinelandii* FdI [37]) is a tryptophan and a tyrosine, respectively (Fig. 2). Both amino acids are nonpolar but the indol nitrogen of tryptophan can hydrogen bond donate, either attracting water to the vicinity of the cluster or forming new NH–S bonds with the cluster. Redox potentials of [Fe-S] clusters are known to be positively increased by the solvent accessibility and by the formation of specific hydrogen bonding [37,39]. Therefore, the higher shift observed for *Dalask*Fd in comparison with *Da*FdIII, associated with the formation of the new [4Fe–4S] centre, can be due to the presence of a tryptophan residue instead of a tyrosine.

3.4. EPR Spectroscopic Data Supporting the Electrochemical Studies

The as-isolated *Dalask*Fd presents an almost isotropic EPR signal at $g \sim 2.02$ typical of $[3Fe\text{–}4S]^{+1}$ clusters, that accounted for 0.8 ± 0.1 spins/molecule, using Cu-EDTA standard (Fig. 6A(a)) [40]. This signal is similar to those observed for other 7 Fe ferredoxins containing [3Fe–4S] and [4Fe–4S] centres, like the *D. africanus* FdIII, but also in the native *D. gigas* FdII which contains only one [3Fe-4S] centre [4,6].

Upon reduction with sodium dithionite ($E = -350$ mV vs. SHE), it is observed the disappearance of the $g = 2.02$ signal and the appearance of a rhombic signal with *g* values of 2.06, 1.94 and 1.90, typical of a reduced $[4Fe\text{–}4S]^{+1}$ cluster with a $S = 1/2$ ground state (Fig. 6A(b)). Spin quantification of this signal yielded 0.9 ± 0.1 spins/molecule indicating that *Dalask*Fd contains approximately a 1:1 ratio between the [3Fe–4S] and the [4Fe–4S] centers per monomer and therefore is a 7Fe ferredoxin, as expected from the electrochemical results discussed above and the primary amino acid sequence analysis.

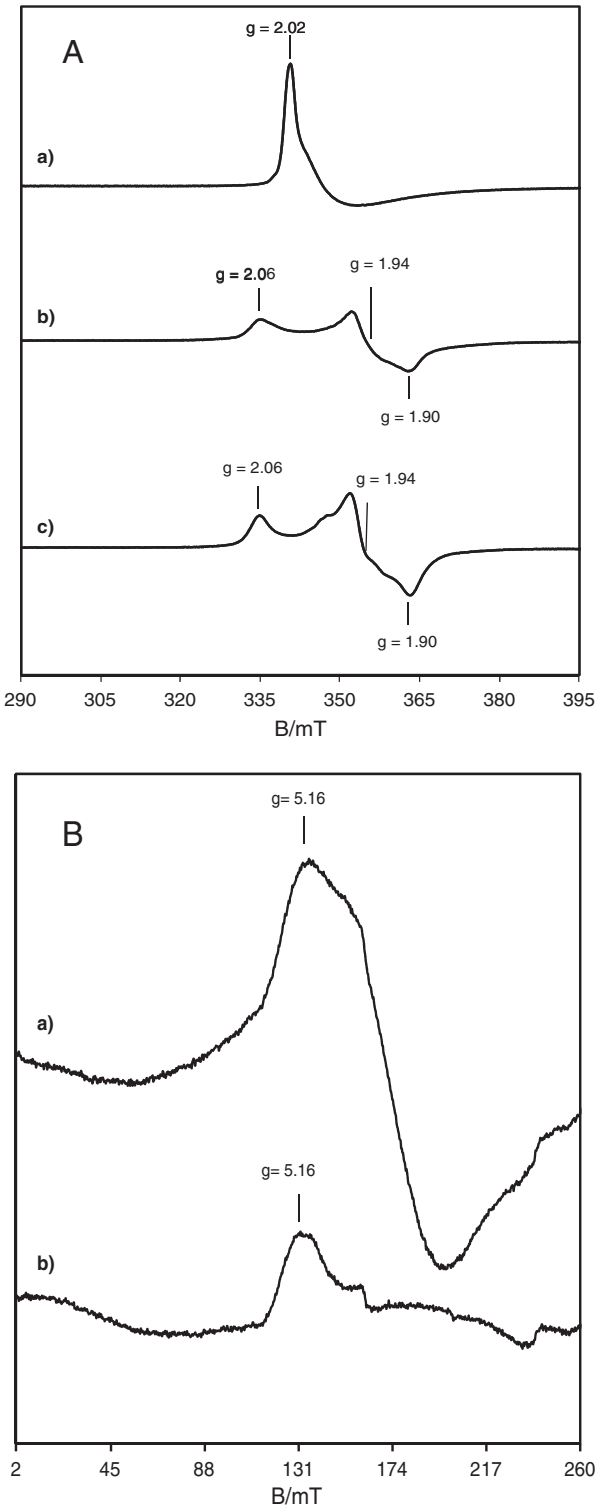

Fig. 6. X-band EPR spectra of 300 μM *Dalask*Fd in Tris-HCl 100 mM, pH 7.6. Panel A: (a) as-purified, (b) reduced with sodium dithionite solution and (c) reduced with Ti(III) citrate solution. EPR conditions were microwave frequency, 9.64 GHz; modulation amplitude, 10 G; temperature, 4.8 K and microwave power, 0.2 mW. Panel B: (a) reduced with sodium dithionite solution and (b) reduced with Ti(III) citrate solution. The EPR conditions were the same as in panel A, except the microwave power, 20 mW. The vertical lines indicate the representative *g*-factors.

At low field it is also possible to observe a resonance at $g = 5.16$ corresponding to a [4Fe–4S] cluster with a ground state of $S = 3/2$ (Fig. 6B(a)). Similar signals have been observed in other 7Fe ferredoxins and were attributed to $[4Fe–4S]^{+1}$ clusters formed by the conversion of $[3Fe–4S]^{+1}$ clusters upon reduction in the presence of iron [6,7]. In this type of ferredoxins the conversion of the [3Fe-4S] cluster into a [4Fe-4S] uses an Aspartate residue instead of a cysteine for the iron coordination. This was confirmed by Bush and co-workers for *Da*FdIII in which it was shown that mutation of the Asp by a Cys residue leads to the disappearance of the low field signal to give two [4Fe–4S] clusters with the same g ~ 2.06 EPR signal [13]. *Dalask*Fd amino acid sequence shows the conserved Asp^{15} residue (Fig. 2), which suggests that the $g = 5.16$ EPR signal is due to $[4Fe–4S]^{1+}$ cluster formed by conversion of part of the $[3Fe–4S]^{0}$ cluster using the adventitious iron present in the solution, since no iron was added.

Further reduction of *Dalask*Fd with titanium citrate ($E = -500$ mV vs. SHE) yields a pronounced decrease in the intensity of the signal of the $S = 3/2$ [4Fe–4S] centre (Fig. 6B(b)), and simultaneously the appearance of additional shoulders (Fig. 6A(c)) around the g_{mid} resonance with respect to spectrum (b) of the same figure. The additional shoulders observed may arise from magnetic interactions between the two clusters, after reduction with titanium citrate.

4. Conclusions

A ferredoxin from *D. alaskensis* was characterized and particular attention was given to the redox properties and control on cluster structures. The protein contains one [3Fe–4S] and one [4Fe–4S] centre. Sequences analysis showed that, as well as the homologous 7Fe ferredoxins *Da*FdIII and *Dv*MFdI, this ferredoxin presents an aspartate residue (Asp^{15}) in the binding motif instead of the usual cysteine. Differential pulse voltammograms exhibited three reversible electrochemical signals, corresponding to the following reduction processes: $[3Fe–4S]^{+1/0}$ ($E^{0'} = -158 \pm 5$ mV); $[4Fe–4S]^{+2/+1}$ ($E^{0'} = -474 \pm 5$ mV); and $[3Fe–4S]^{0/-2}$ ($E^{0'} = -660 \pm 5$ mV). A proton uptake by the $[3Fe–4S]^{0}$ centre was detected ($pK'_{red} = 5.1 \pm 0.1$), whereas the $[4Fe–4S]^{+2/+1}$ centre showed to be pH independent. Further reduction of the $[3Fe–4S]^{0}$ centre is a cooperative two-electron process accompanied by the binding of two protons. The $[3Fe–4S]^{0}$ cluster can be converted into a new [4Fe–4S] in the presence of Fe(II) ions, with the potential of the original $[4Fe–4S]^{+2/+1}$ cluster being positively shifted (*ca.* 70 mV) during the conversion process.

EPR spectroscopy fully supported the electrochemical observations. The EPR spectra showed a typical nearly isotropic signal at $g = 2.02$, characteristic of the $[3Fe–4S]^{+1}$ cluster (as-isolated protein), and a rhombic signal upon reduction with sodium dithionite, which is characteristic of the $[4Fe–4S]^{+1}$ cluster with $S = 1/2$. Simultaneously, another signal at low field is observed ($g = 5.16$, $S = 3/2$), which is attributed to the presence of a new $[4Fe–4S]^{+1}$ cluster. The latter results from the reaction of the reduced $[3Fe–4S]^{0}$ centre with adventitious iron, using the aspartate residue (Asp^{15}) as the fourth ligand. Reduction with Ti(III) citrate caused a strong decrease in the intensity of the signal at $g = 5.16$, as well as the appearance of spin-spin couplings between the two [4Fe–4S] centres, suggesting that they are interacting.

Given that the metabolic environment in sulphate reducing bacteria is extremely reductive, the cluster interconversion acquires biological significance. Structural control, depending on the type of cluster and on the nature of the amino acids residues present in its surroundings, affects the reduction potentials of the centres and determines the electron transfer properties of these proteins.

Acknowledgments

This research was supported by FCT (Fundação para a Ciência e Tecnologia) grant SFRH/BPD/14938/2004 (to R. G.). P. M. P. S. and M. S. P. C. would like to thank programme Ciência 2007 (FCT-MCTES). C.D.B. is a member of CONICET-Argentina.

References

[1] H. Beinert, R.H. Holm, E. Münck, Iron–sulfur clusters: nature's modular, Multipurpose Structures Science 277 (1997) 653–659.
[2] M.K. Johnson, Iron–sulfur proteins: new roles for old clusters, Curr. Opin. Chem. Biol. 2 (1998) 173–181.
[3] D.C. Johnson, D.R. Dean, A.D. Smith, M.K. Johnson, Structure, function, and formation of biological iron–sulfur clusters, Annu. Rev. Biochem. 74 (2005) 247–281.
[4] F.A. Armstrong, S.J. George, R. Cammack, E.C. Hatchikian, A.J. Thomson, Electrochemical and spectroscopic characterization of the 7Fe form of ferredoxin III from *Desulfovibrio africanus*, Biochem. J. 264 (1989) 265–273.
[5] M. Ogata, S. Kondo, N. Okawara, T. Yagi, Purification and characterization of ferredoxin from *Desulfovibrio vulgaris* Miyazaki, J. Biochem. Tokyo 103 (1988) 121–125.
[6] J.J.G. Moura, I. Moura, T.A. Kent, J.D. Lipscomb, B.H. Huynh, J. LeGall, A.V. Xavier, E. Munck, Interconversions of [3Fe–3S] and [4Fe–4S] Clusters, J. Biol. Chem. 257 (1982) 6259–6267.
[7] C. Moreno, A.L. Macedo, I. Moura, J. LeGall, J.J. Moura, Redox properties of Desulfovibrio gigas [Fe_3S_4] and [Fe_4S_4] ferredoxins and heterometal cubane-type clusters formed within the [Fe_3S_4] core. Square wave voltammetric studies, J. Inorg. Chem. 53 (1994) 219–234.
[8] J.N. Butt, F.A. Armstrong, Voltammetry and adsorbed redox enzymes: mechanisms in the potential dimension, in: Hammerish, J. Ulstrup (Eds.), Bioinorganic Electrochemistry, 2008, pp. 91–128.
[9] M.M. Correia dos Santos, P.M. Paes de Sousa, M.L. Simões Gonçalves, L. Krippahl, J.J.G. Moura, É. Lojou, P. Bianco, Electrochemical studies on small electron transfer proteins using membrane electrodes, J. Electroanal. Chem. 541 (2003) 153–162.
[10] S.J. George, F.A. Armstrong, E. Hatchikian, A. Thomson, Electrochemical and spectroscopic characterization of the conversion of 7Fe into 8Fe form of ferredoxin III from *Desulfovibrio africanus*, Biochem. J. 264 (1989) 275–284.
[11] F.A. Armstrong, J. Butt, S.J. George, E. Hatchikan, A. Thomson, Evidence for reversible multiple redox transformations of [3Fe–4S] clusters, FEBS Lett. 259 (1989) 15–18.
[12] J. Busch, J. Breton, B.M. Bartlett, R. James, E. Hatchikian, A. Thomson, Expression in *Escherichia coli* and characterization of a reconstituted recombinant 7Fe ferredoxin from *Desulfovibrio africanus*, Biochem. J. 314 (1996) 63–71.
[13] J. Busch, J. Breton, B.M. Bartlett, F.A. Armstrong, R. James, A. Thomson, [3Fe-4S] <——> [4Fe-4S] cluster interconversion in *Desulfovibrio africanus* ferredoxin III: properties of an Asp14 –>Cys mutant, Biochem. J. 323 (1997) 95–102.
[14] M.J. Feio, V. Zinkevich, I.B. Beech, E. Llobet-Brossa, P. Eaton, J. Schmitt, J. Guezennec, *Desulfovibrio alaskensis* sp. nov., a sulphate-reducing bacterium from a soured oil reservoir, Int. J. Syst. Evol. Microbiol. 54 (2004) 1747–1752.
[15] S. Chhabra, Q. He, K. Huang, S. Gaucher, E.J. Alm, Z. He, M.Z. Hadi, T.C. Hazen, J.D. Wall, J. Zhou, A.P. Arkin, A.K. Singh, Global analysis of heat shock response in *Desulfovibrio vulgaris* Hildenborough, J. Bacteriol. 188 (2006) 1817–1828.
[16] J.D. Wall, L.R. Krumholz, Uranium reduction, Annu. Rev. Microbiol. 60 (2006) 149–166.
[17] S.F. Altschul, W. Gish, W. Miller, E.W. Myers, D.J. Lipman, Basic local alignment search tool, J. Mol. Biol. 215 (1990) 403–410.
[18] J.D. Thompson, T.J. Gibson, F. Plewniak, F. Jeanmougin, D.G. Higgins, The CLUSTAL_X windows interface: flexible strategies for multiple sequence alignment aided by quality analysis tools, Nucleic Acids Res. 25 (1997) 4876–4882.
[19] L.C. Seefeldt, S.A. Ensign, A continous, spectrophotometric activity assay for nitrogenase using the reductant titanium(III) citrate, Anal. Biochem. 221 (1994) 379–386.
[20] E. Hatchikian, M. Bruschi, Characterization of a new type of ferredoxin from *Desulfovibrio africanus*, Biochim. Biophys. Acta 634 (1981) 41–51.
[21] J.J.G. Moura, A.L. Macedo, P.N. Palma, in: H.D. Peck, J. LeGall Jr. (Eds.), Methods in Enzymology, Ferredoxins, Academic Press Inc, 1994, pp. 165–188.
[22] R.C. Conover, A.T. Kowal, W.G. Fu, J.B. Park, S. Aono, M.W. Adams, M.K. Johnson, Spectroscopic characterization of the novel iron-sulfur cluster in *Pyrococcus furiosus* ferredoxin, J. Biol. Chem. 265 (1990) 8533–8541.
[23] Y. Minami, S. Wakabayashi, K. Wada, H. Matsubara, L. Kerscher, D. Oesterhelt, Amino acid sequence of a ferredoxin from thermoacidophilic archaebacterium, *Sulfolobus acidocaldarius*. Presence of an N6-monomethyllysine and phyletic consideration of archaebacteria, J. Biochem. 97 (1985) 745–753.
[24] S. Wakabayashi, N. Fujimoto, K. Wada, H. Matsubara, L. Kerscher, D. Oesterhelt, Amino acid sequence of a ferredoxin from thermoacidophilic archaebacteria, *Thermoplasma acidophilum*, FEBS Letters 162 (1983) 21–24.
[25] A.J. Bard, L.R. Faulkner, Electrochemical Methods, Fundamentals and Applications, second ed. Wiley, New York, 2001.
[26] C. Tanford, Physical Chemistry of Macromolecules, Wiley, New York, 1961.
[27] M. Asso, O. Barki, B. Guigliarelli, T. Yagi, P. Bertrand, EPR and redox characterization of ferredoxins I and II from *Desulfovibrio vulgaris* Miyazaki, Biochem. Biophysic. Res. Communica. 221 (1995) 198–204.
[28] J.L.C. Duff, J.L. Breton, J.N. Butt, F.A. Armstrong, A.J. Thomson, Novel redox chemistry of [3Fe–4S] clusters: electrochemical characterization of the All-Fe(II) form of the [3Fe–4S] cluster generated reversibly in various proteins and its spectroscopic investigation in *Sulfolobus acidocaldarius* ferredoxin, J. Am. Chem. Soc. 118 (36) (1996) 8593–8603.
[29] G.R. Moore, G.W. Pettigrew, Cytochromes c: evolutionary, structural and physicochemical aspects, Springer, Berlin, 1990.
[30] F.A. Armstrong, S.J. George, A.J. Thomson, M.G. Yates, Direct electrochemistry in the characterization of redox proteins: novel properties of *Azotobacter* 7Fe ferredoxin, FEBS Lett. 234 (1988) 107–110.
[31] S.E. Iismaa, A.E. Vázquez, G.M. Jensen, P.J. Stephens, J.N. Butt, F.A. Armstrong, B.K. Burgess, Site-directed mutagenesis of *Azotobacter vinelandii* ferredoxin I, J. Biol. Chem. 266 (1991) 21563–21571.
[32] J.L. Breton, J.L. Duff, J.N. Butt, F.A. Armstrong, S.J. George, Y. Pétillot, E. Forest, G. Schäfer, A.J. Thomson, Identification of the iron-sulfur clusters in a ferredoxin from the archaeon *Sulfolobus acidocaldarius*. Evidence for a reduced [3Fe–4S] cluster with pH-dependent electronic properties, Eur. J. Biochem. 233 (1995) 937–946.
[33] C.D. Stout, Crystal strucutures of oxidized and reduced *Azotobacter vinelandii* ferredoxin at pH 8 and 6, J. Biol. Chem. 268 (1993) 25920–25927.
[34] D. Bentrop, I. Bertini, M. Borsari, Cosenza,C Luchinat, Y. Niikura, A refined model for [Fe_3S_4]^0 clusters in proteins, Angew. Chem. Int. Ed. 39 (2000) 3620–3622.
[35] B. Shen, L.L. Martin, J.N. Butt, F.A. Armstrong, C.D. Stout, G.M. Jensen, P.J. Stephens, G.N. La Mar, C.M. Gorst, B.K. Burgess, *Azotobacter vinelandii* ferredoxin I. Aspartate 15 facilitates proton transfer to the reduced [3Fe–4S] cluster, J. Biol. Chem. 268 (1993) 25928–25939.
[36] R. Camba, L.M. Yean-Sung Jung, B.K. Hunsicker-Wang, C.D. Burgess, J. Stout, Hirst F.A. Armstrong, Mechanisms of redox-coupled proton transfer in proteins: role of the proximal proline in reactions of the [3Fe–4S] cluster in *Azotobacter Vinelandii* ferredoxin I, Biochem. 42 (2003) 10589–10599.
[37] K. Chen, C.A. Bonagura, G.J. Tilley, J.P. McEvoy, Jung Yean-Sung, F.A. Armstrong, C.D. Stout, B.K. Burgess, Crystal structures of ferredoxin variants exhibiting large changes in [Fe–S] reduction potential, Nat. Struct. Biol. 9 (2002) 188–192.
[38] Z. Dauter, K.S. Wilson, L.C. Sieker, J. Meyer, J.M. Moulis, Atomic resolution (0.94 A) structure of *Clostridium acidurici* ferredoxin. Detailed geometry of [4Fe–4S] clusters in a protein, Biochem. 36 (1997) 16065–16073.
[39] P.J. Stephens, D.R. Jollie, A. Warshel, Protein control of redox potentials of iron–sulfur proteins, Chem. Rev. 96 (1996) 2491–2513.
[40] T.A. Kent, B.H. Huynh, E. Münck, Iron–sulfur proteins: spin-coupling model for three-iron clusters, Proc. Natl. Acad. Sci. USA 77 (1980) 65–6574.